CHAPTER IV

RESULTS AND DISCUSSION

4.1 Characterization of Synthesized Polyaniline

4.1.1 Fourier-Transform Infrared Spectrometer (FT-IR)

The polymerization of aniline was designed to be as simple as possible. The polyemeraldine salt was first synthesized by the oxidation of aniline hydrochloride with ammonium peroxydisulfate in aqueous solution at room temperature. Then, the green precipitate of polyemeraldine salt was converted to blue powder of polyemeraldine base by ammonium hydroxide. The reaction can be summarized in Figure 4.1. The polyemeraldine base can be dissolved in organic solvent and blended with polyvinyl alcohol.

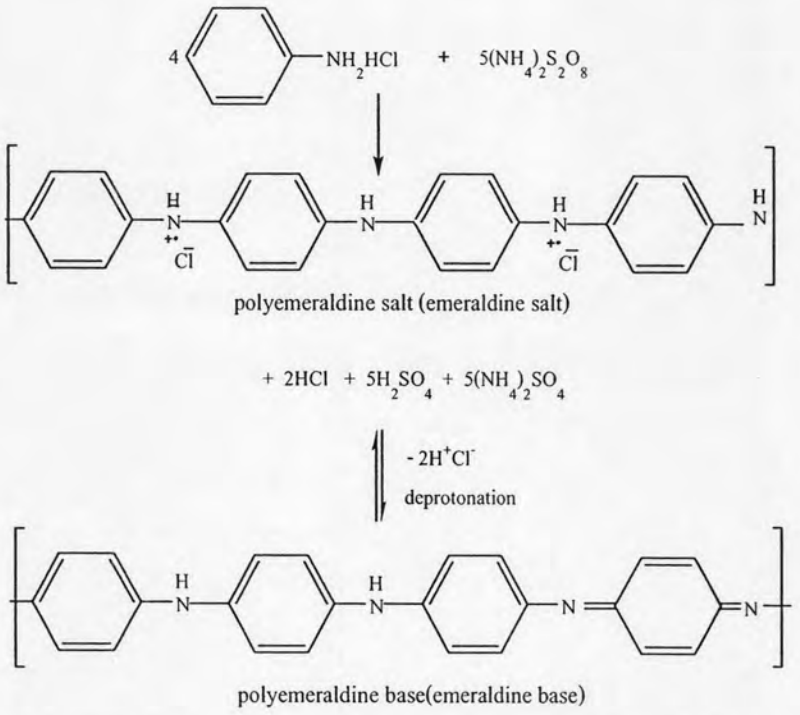

Figure 4.1 Synthesis of Polyemeraldine base (PANi-EB).

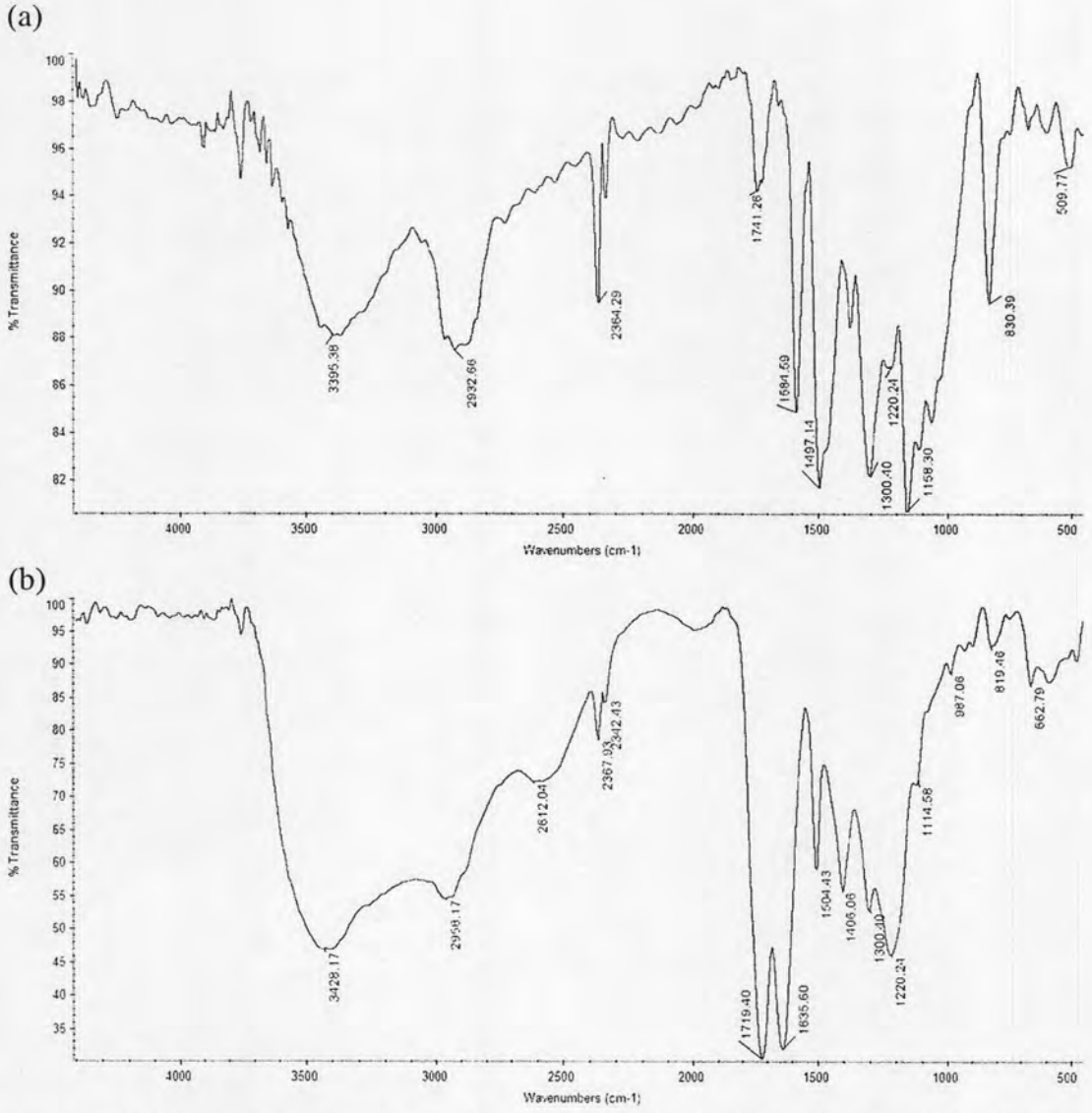

Figure 4.2 The IR spectrum of synthesized of (a) PANi-EB and (b) PANi-citric acid.

The PANi-EB was characterized by FT-IR. The IR spectrum of synthesized PANi-EB was shown in Figure 4.2 (a). All the peak locations, related to the chemical bonds, were tabulated in Table 4.1. The characteristic bands of PANi were observed at 3395.38 cm^{-1}, 1584.59 cm^{-1}, 1497.14 cm^{-1}, 1300.40 cm^{-1}, 1158.30 cm^{-1} and 830.39cm^{-1} corresponding to N-H stretching of aromatic amine, C=C stretching of quinoid imine, C=C stretching of benzenoid diamine, C-N-C stretching of a secondary of aromatic amine for both quinoid and benzenoid segments, vibration mode of quinoid ring, out of plane bending of para-substitute of aromatic benzene ring, respectively.

Table 4.1 The IR characteristic peaks of the synthesized PANi-EB

Wavenumber (cm^{-1})	Functional group
3395.38	N-H stretching of aromatic amine
2932.66	C-H stretching of the aromatic ring
1584.59	C=C stretching of quinoid imine
1497.14	C=C stretching of benzenoid diamine
1300.40	C-N-C stretching of a secondary of aromatic amine for both quinoid and benzenoid segments
1158.30	Vibration mode of quinoid ring
830.39	Out of plane bending of para-substitute of aromatic benzene ring

Table 4.2 The IR characteristic peaks of the synthesized PANi-citric acid

Wavenumber (cm^{-1})	Functional group
3428.17	N-H stretching of aromatic amine
3300-2500	O-H of carboxylic acid
2800-2200	Overtone of carboxylic acid
1719.40	C=O stretching of carboxylic acid
1635.60	-COO- stretching
1406.06, 1220.24	-C-OH stretching and –C-O in-plane bending
1300.40	C-N-C stretching of a secondary of aromatic amine
987.06	-OH out-of-plan bending of carboxylic acid

The IR spectrum of polyemeraldine base doped with citric acid (PANi-citric acid) was shown in Figure 4.2 (b) and tabulated in Table 4.2. The PANi-citric acid shows strong peak of carbonyl (-C=O) stretching at 1719.40 cm^{-1} and carboxylate anion (-COO-) stretching at 1635.60 cm^{-1}, typical features of carboxyl group of citric acid. Moreover, the peaks at 1220.24 and 1406.06 cm^{-1} is due to the -C-O stretching and -C-OH in-plane bending, respectively, indicating that PANi is conductive and is in the form of high doped emeraldine salt.

4.2 Fiber formation and morphology of electrospun citric acid doped PANi-PVA mats

From preliminary study, electrospinning of citric acid doped PANi-PVA solution without syringe pump had given highly unstable fibers and also difficult for continuous spinning. Drying and clogging of solution at the end of the needle tip during spinning caused the fibers form with blobs structural defects. In order to form the uniform fibers, the jets must be ejected from the needle tip with constant flow rate, and thus the syringe pump was applied to improve the electrospinnability of citric acid doped PANi-PVA.

When only citric acid doped PANi solution was electrospun, no fiber formed because the viscosity and surface tension of the solution were not high enough to maintain a stable drop at the end of the needle tip. PVA could be electrospun and there were plenty of literatures were evident the easy spinability of PVA nanofibers. Therefore, the PVA was used to assist the fiber formation of PANi.

The morphology and properties of electrospun fibers were depended on the various parameters, mainly solution properties and electrospinning process. The solution properties were concentration, viscosity, conductivity and surface tension of polymer solution. Factor of electrospinning process were diameter of needle, electric potential, distance between needle and collection screen, and flow rate of solution. To optimize the condition for electrospinning of PANi-PVA mats, SEM photographs and diameter of fibers were evaluated.

4.2.1 Effect of needle diameter

The effect of needle diameter on the electrospun PANi-PVA mats has been studied for two different needle sizes, internal needle diameter of 0.55 and 0.80 mm, as shown in Figure 4.3. The average diameter of PANi-PVA fibers using needle diameter of 0.55 mm was 589 nm which is smaller than those using needle diameter of 0.80 mm (709 nm) and more uniformed (small standard deviation (SD) value). The

decrease of fiber diameter caused by the decrease of droplet located at the needle tip. In the other words, a surface tension of droplet was increased. Therefore, at the same electric potential supplied, a greater columbic force was required to cause jet initiation. As a result, the acceleration of jet decreases, and thus allowing more time for the solution to be stretched and elongated before collected. Then, 0.55 mm of needle diameter was selected for the electrospinning process.

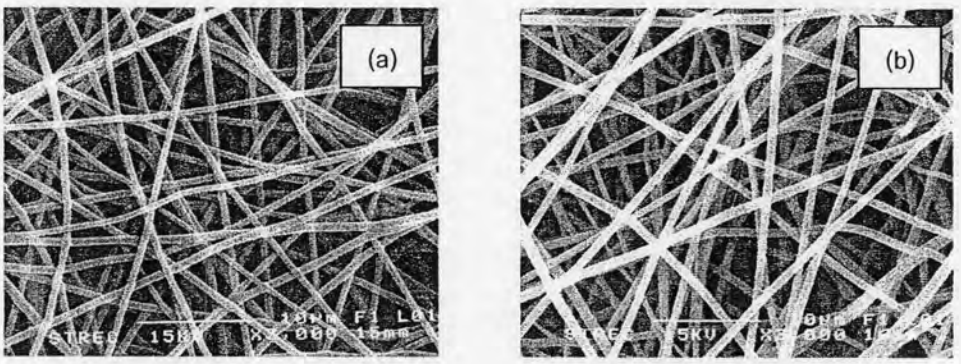

Average 589 ± 31 nm Average 709 ± 148 nm

Figure 4.3 SEM of electrospun mat formed at needle diameter of (a) 0.55 mm and (b) 0.80 mm. Original magnifications 3,000x (flow rate of 15 μL/min, distance between needle and collection screen of 25 cm and electric potential of 15 kV).

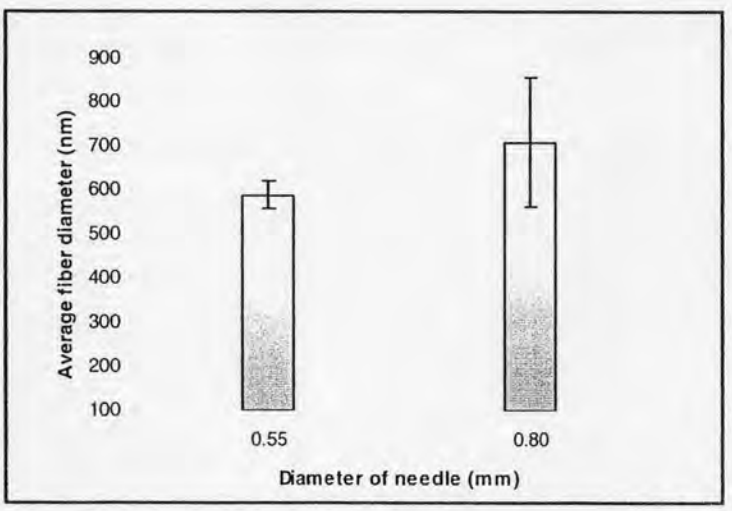

Figure 4.4 Average diameters of electrospun fibers at needle diameter of needle of 0.55 and 0.80 mm.

4.2.2 Effect of solution flow rate

Figure 4.5 and 4.6 shows SEM photographs and average diameter of PANi-PVA electrospun mats at various flow rates. Normally, increasing flow rate of polymer solution will decrease electrostatic density and resulting in the increased of fiber diameter. However, in this study, changing the flow rate from 10 to 15 μL/min did not significantly affect diameter of fibers. Therefore, the optimum solution flow rate was selected at 15 μL/min for fast electrospinning process.

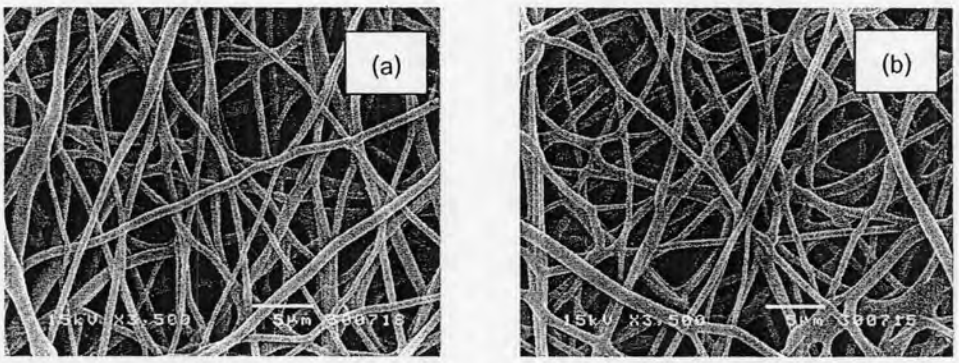

Average 587 ± 130 nm Average 597 ± 108 nm

Figure 4.5 SEM of electrospun mat formed of (a) 10 μL/min and (b) 15 μL/min. Original magnifications 3,500x (distance between needle and collection screen of 10 cm and electric potential of 10 kV).

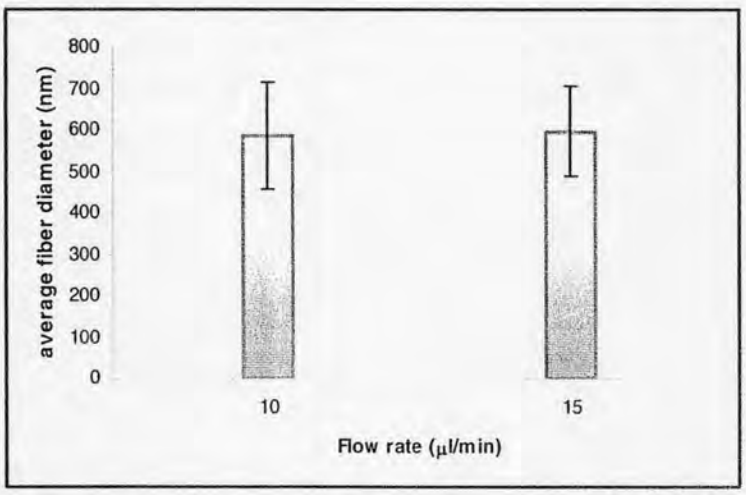

Figure 4.6 Average diameters of electrospun fibers at flow rate of 10 and 15 μL/min.

4.2.3 Effect of electrical potential and distance between needle and collection screen

The effects of applied electric potential on morphology and diameter of fiber need to be considered together with distance between the needle and the collection screen [54] because change of distance between the needle and the collection screen influences directly electric field generated by electric potential.

Figure 4.7 shows the results of SEM observation at different combinations of distance between the needle and the collection screen and electric potential on electrospinning of PANi-PVA. Generally, the increasing in electric potential allowed the polymer jet to discharge with a greater electrostatic repulsion that caused it to undergo higher levels of drawing stress. This resulted in the decrease of the fiber diameter and also the bead on fiber decreases. However, in this work, when changing the electric potential from 10 kV to 30 kV (keeping other parameters constant), the average diameter of fiber was in the range 400–700 nm with broad diameter distribution. The diameter of electrospun fibers did not follow what described above when increased electric potential. One possible reason for this could be the effect of polymer solution which has high viscosity and resist to the electric field. Therefore, the diameter of the fibers did not decrease. Moreover, at the distance of 10 cm, when increasing the electric potential, beaded fibers were clearly observed. The amount of these beaded fibers was found to increase when electric potential increased in the rage of 10 to 20 kV, with the shuttle-shape beads on fiber. As electric potential increased from 25 to 30 kV, the bead features became overlaps among the fibers. The apparent discrepancy in the reported effects of electric potential on diameter of fiber noted above is likely due to different flow rate, distance and concentrations used in the different studies [55]. Electric potential induced instability of the Taylor's cone may also result in changes in diameter of fibers. At constant distance and flow rate, high electric potential may result in the Taylor's cone receding into the needle and the spinning occurs from within the needle. The nanofibers formed were uneven and beaded. Moreover, Deitzel et al. investigated the formation of beads and found out that the spinning electric potential largely influences the formation of

beads, the bead defect density increased with increasing electric potential. For the distance of 15, 20 and 25 cm in various the electric potential at 10, 15 and 20 kV; smooth, regular and straight electrospun fibers were obtained. Whereas, slightly bead fibers and overlaps among fibers were observed with increasing electric potential was too high, the electric potential at 25 and 30 kV. Various distances between the needle and the collection screen were set between the range of 10 and 25 cm (keeping each electric potential constant). Varying the distance between the needle and the collection screen will have a direct influence on both the flight time and the strength of electric field. The electrospinning jet must have more time for the solvent to be evaporated. In this work, beads were observed to form when distance was low (10 cm). When the distance between the needle and the collection screen is reduced, the jet will have a shorter distance to travel before it reaches the collector and might result in the increase of electric field between the needle tip and the collector. Decreasing the distance has the same effect as increasing the electric potential supplied and this will cause an increased in the electric field and also will increase the acceleration of the jet to the collector. As a result, they may not have enough time for the solvents to evaporate when it reaches the collector. Therefore, diameter of fiber has bead feature appeared. As distance was 15, 20 and 25 cm (electric potential from 10 to 20 kV), the electrospun fibers became regular, uniform, and straighter with increase the distance between needle and collection screen. However, the uniform fiber structure turned out to be irregular when the electric potential is too much as in SEM of 25 cm 20 kV. Increasing the distance between the needle and the collector results in a decreased in the average diameter fiber. The longer distance means that there is a longer flight time for the solution to be stretched before it is reached on the collector. However, in some case, at a longer distance, the fiber diameter increased. This is due to the decrease in the electrostatic field resulting in less stretching of the fibers. When the distance is too large, no fibers are reached on the collector. Therefore, it seems that there is an optimal electrostatic field below which the stretching of the solution will decrease resulting in increased fiber diameters. The diameter of fibers was reported as the average values with standard deviation in Figure 4.8 and 4.9 while raw data were summarized in Table 4.3.

The SEM of 20 cm, 10 kV, 20 cm 15 kV, 25 cm 10 kV and 25 cm 15 kV were shown a satisfactory fiber mats, because regular and straight fibers were formed and bead was not found. However, at the distance of 25 cm 15 kV, the fine fibers can be produced and the diameter distribution of fibers was less than those in other conditions. Therefore, the electric potential and distance between needle and collection screen were optimized to 25cm and 15 kV.

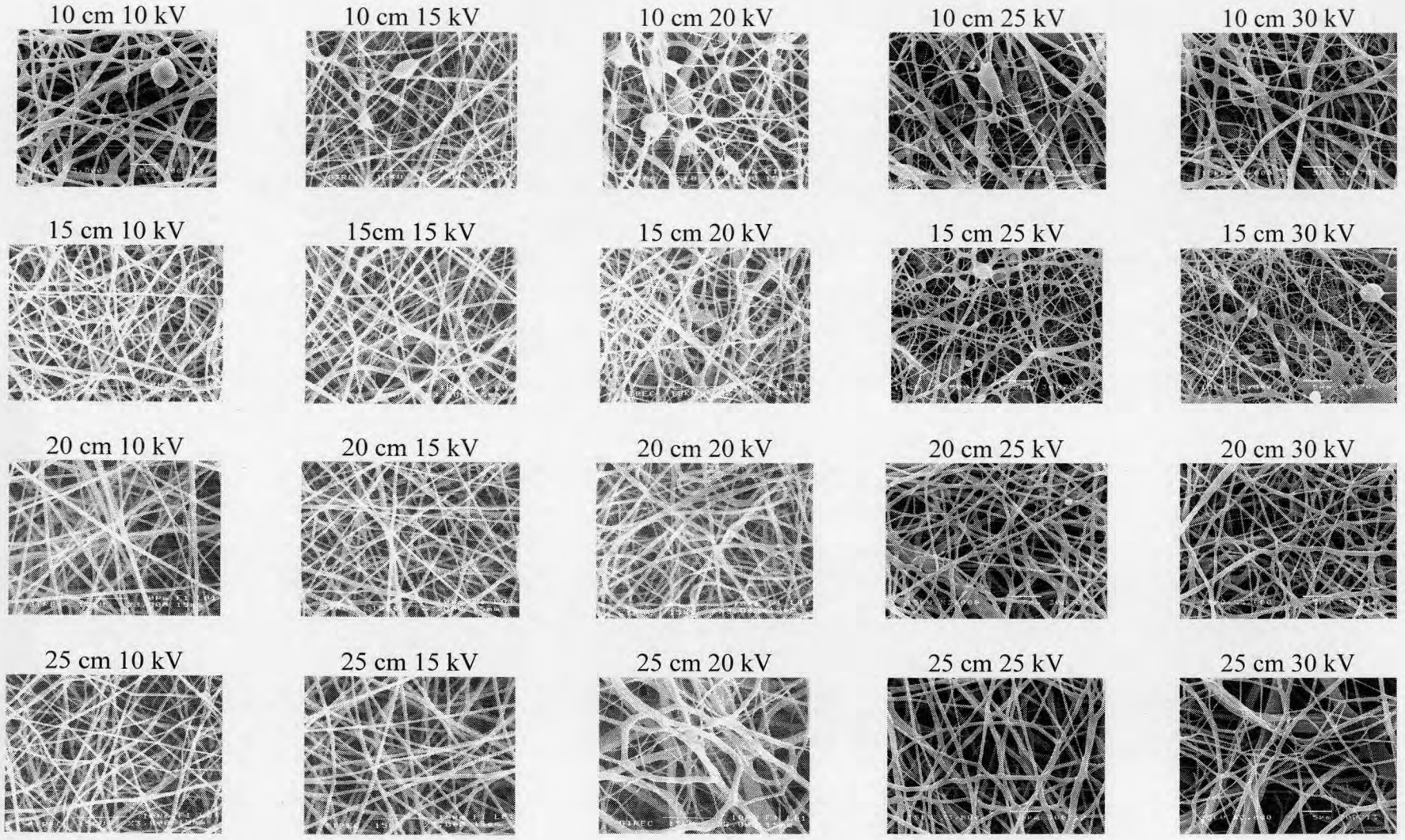

Figure 4.7 SEM image of electrospun citric acid doped PANi-PVA mats. Original magnifications 3,000x.

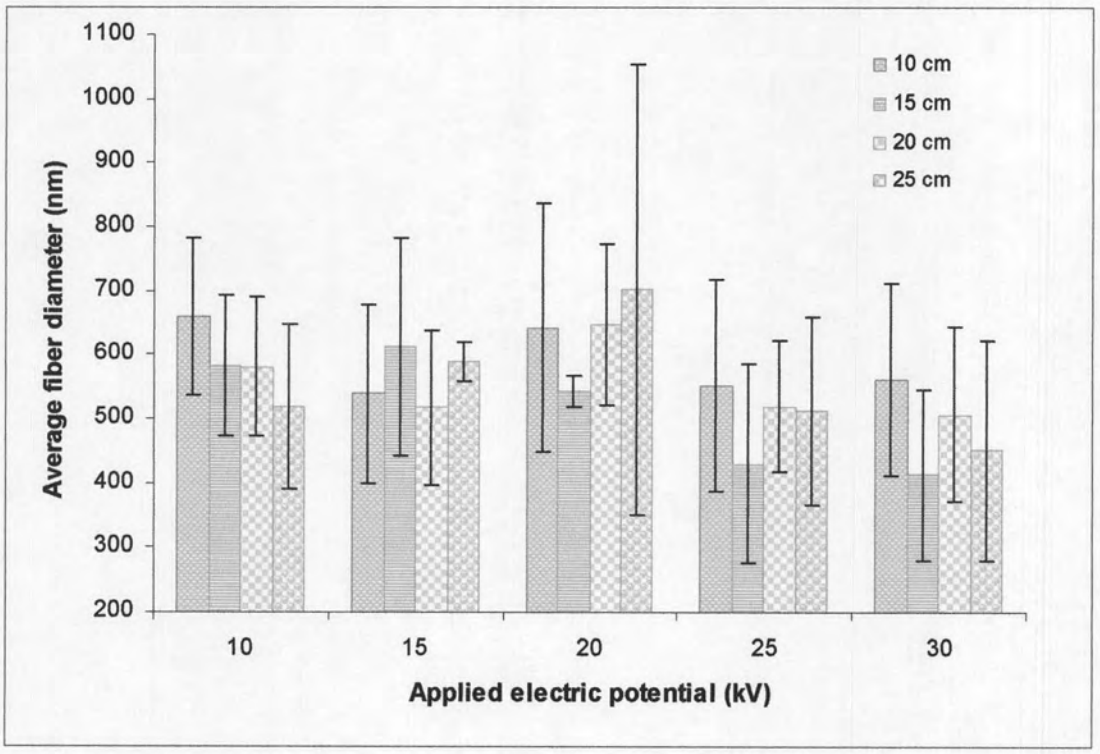

Figure 4.8 Average diameters of electrospun fibers at various electric potential and distances between the needle and the collection screen.

Table 4.3 The electrospinning conditions of PANi-PVA

Concentration (wt/v %)	Solvents	Flow rate (μl/min)	Distance (cm)	Potential (kV)	Formation	Average diameter of fiber (nm)
2%PANi-10%PVA	N-methyl-2-pyrrolidone	15	10	10	Bead fibers	660 ± 122
				15	Bead fibers	539 ± 139
				20	Bead fibers	642 ± 193
				25	Blob fibers	552 ± 164
				30	Blob fibers	562 ± 149
2%PANi-10%PVA	N-methyl-2-pyrrolidone	15	15	10	Fibers	582 ± 110
				15	Fibers	612 ± 169
				20	Fibers	543 ± 124
				25	Bead fibers	431 ±155
				30	Bead fibers	413 ± 133
2%PANi-10%PVA	N-methyl-2-pyrrolidone	15	20	10	Fibers	580 ± 108
				15	Fibers	518 ± 121
				20	Fibers	648 ± 125
				25	Slight bead fibers	520 ± 102
				30	Fibers	507 ± 136
2%PANi-10%PVA	N-methyl-2-pyrrolidone	15	25	10	Fibers	518 ± 129
				15	Fibers	589 ± 31
				20	Fibers	702 ± 353
				25	Fibers	512 ± 146
				30	Fibers	450 ± 171

4.3 Ammonia sensing

4.3.1 Electrical of resistance of electrospun citric acid doped-PANi-PVA mats

In conventional PANi doped with HA type acid such as HCl, the sensing mechanism was governed by the protonation/deprotonation phenomena. The resistance was then increased when exposed to ammonia. The resistance change in PANi has been explained on the basis of the formation of energetically ammonium ion (NH_4^+) at N^+-H adsorption centre leading to a rise in the resistance on exposure to ammonia [8]. The same ammonium ion decomposed back into ammonia leaving out the proton on the adsorption site in the air environment. However, acrylic acid had been used as a dopant and its response was contrast with that of the conventional trend. The resistance of acrylic acid doped PANi was decreased when exposed to ammonia vapors. This behavior could be interpreted by considering the interaction of NH_3 with the dopant acrylic acid. In the ammonia vapor, NH_3 molecules could attack with two adsorption sites: -N^+H- sites originated from HCl molecules present during polymerization reaction and acrylic acid molecules trapped in polymeric chains. As seen before, NH_3 adsorption onto -N^+H- sites leads to an increase of resistance. On the contrary, NH_3 molecule might take up a hydrogen from acrylic acid forming NH_4^+ which creates -COO^- anion in the polymer chain and leaving a conduction site, leading to the decrease in the material resistance [14]. As the responses observed in the present case, the resistance change were similar to that of acrylic acid-doped PANi. The resistance of electrospun citric acid doped PANi-PVA mats was immediately decreased when exposed to ammonia. The change of resistance of PANi-PVA electrospun mats sensor was in the range 20^6 Ω and 30^6 Ω when exposed to 90 ppm of NH_3 gas. The decreasing of resistance on exposure to ammonia could be probably the interaction of NH_3 with the dopant citric acid. Like acrylic acid doped, ammonia could attack two adsorption sites. The first site was the protonation of PANi chain at N^+-H. Another site was the protonation of free citric acid at carboxylic sites. The latter protonation creates -COO^- anion in the polymeric chain simultaneously leaving one site free for conduction, hence, the resistance decreased. In overall, the

resistance decrease of electrospun citric acid doped PANi-PVA mats imparted from the domination of NH_3 attraction at carboxylic site when exposed to NH_3 as shown in Figure 4.9. Moreover, the resistance of electrospun mats also correlated with the IR characterization of citric acid doped PANi before and after exposed to NH_3.

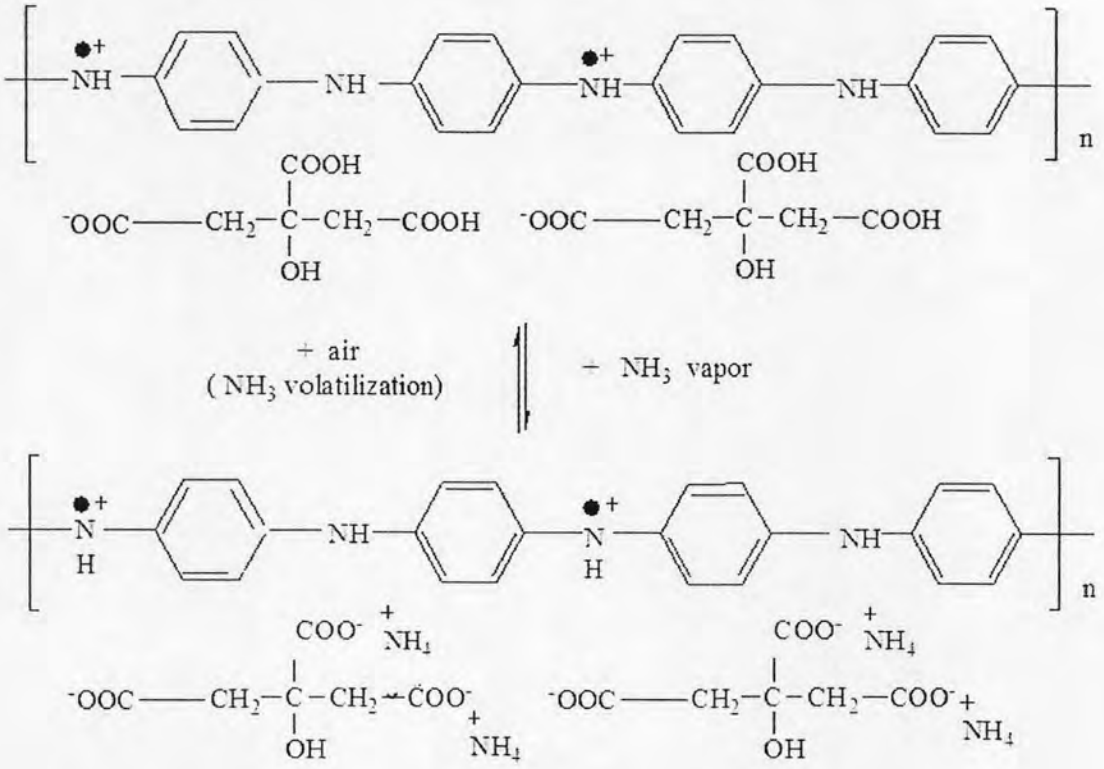

Figure 4.9 Proposed the mechanism of electrospun citric acid doped PANi-PVA mats for ammonia sensing.

The IR spectrum of PANi doped with citric acid before and after exposed to NH_3 was shown in Figure 4.10 (a) and (b), respectively. Due to ammonia molecule possibly taking up proton from carboxylic group of citric acid, this lead to the increase of peak intensity of carbonyl (-C=O) stretching at 1700 cm^{-1}, carboxylate anion (-COO-) stretching at 1642.88 cm^{-1} and the peaks at 1220.24 is due to the -C-O stretching. Besides, the peaks at 1402.42 cm^{-1} is due to the N-O stretching of ammonium acetate, indicating that NH_3 could be the protonated at carboxylic group of citric acid, and then form ammonium acetate on polymer chain.

(a)

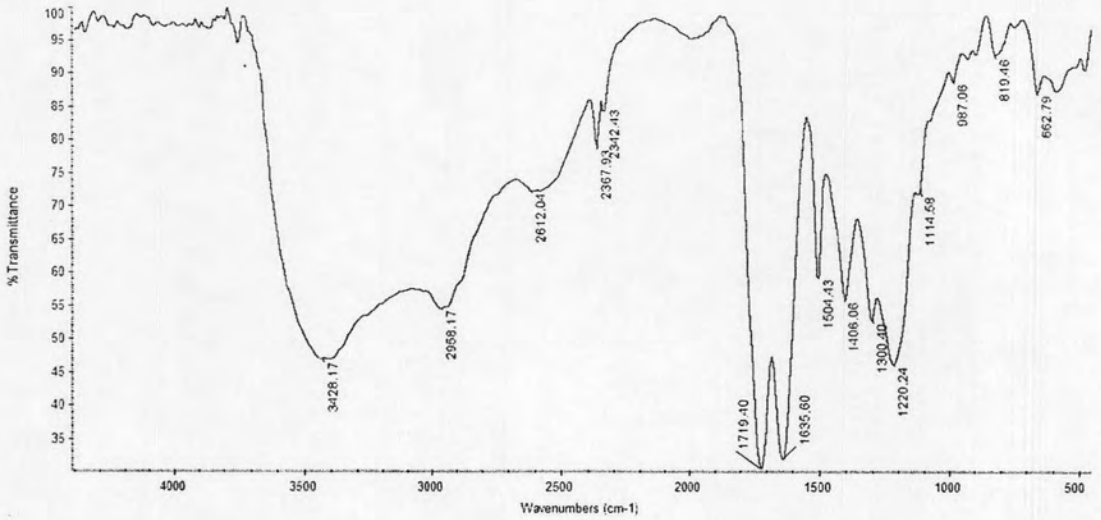

(b)

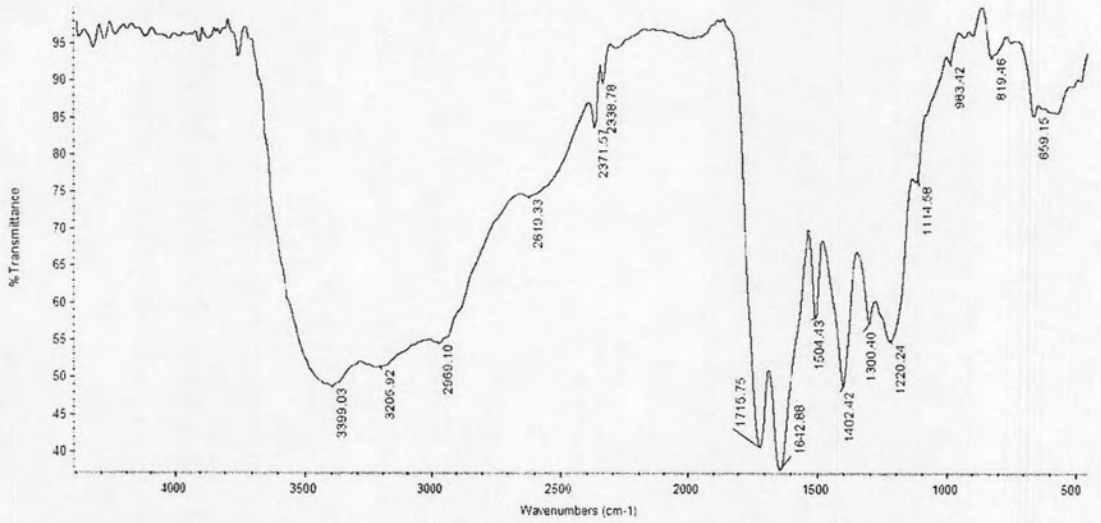

Figure 4.10 The IR spectrum of citric acid doped PANi (a) before exposed to NH_3 and (b) after exposed to NH_3.

4.3.2 Effect of PANi concentration

Among several parameters, the concentration which can imply to viscosity of the electrospinning solution was one of the most effective variables to control the fiber morphology and diameter. In this work, percent of PANi was varied from 1 to 6 % wt/v because concentrations higher than 6% wt/v, PANi did not dissolve in NMP and was over the limit of solubility [61]. The morphology of electrospun fibers observed at various percent of PANi was similar, which was regular as shown in Figure 4.11. Average fiber diameter was summarized in Figure 4.12. The result showed that no significant change of electrospun fiber diameter measured in the experiment. The PANi concentration has no effect on the formation of fiber, because main component of polymer solution was PVA, the percent of PANi in all ratio is considerably small comparing to that of PVA. This would make the viscosity of the overall polymer solutions unchanged at any percent.

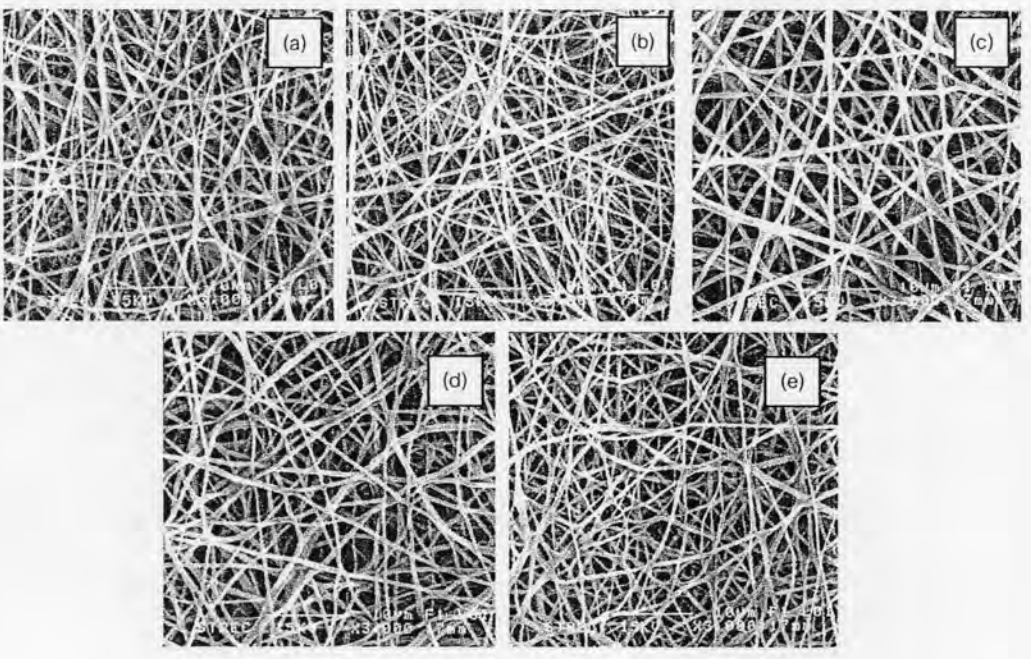

Figure 4.11 SEM of PANi:PVA electrospun mats formed with PANi of (% wt/v) (a) 2, (b) 3, (c) 4, (d) 5, and (e) 6 at solution flow rate of 15 μL/min, distance between needle and collection screen of 25 cm and electric potential of 15 kV. Original magnifications are 3,000x.

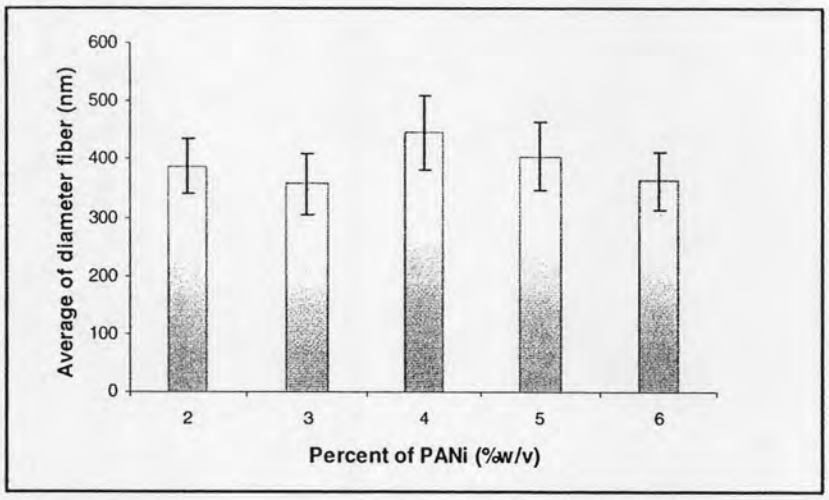

Figure 4.12 Average diameters of electrospun fibers at various percent PANi.

Table 4.4 Resistance of PANi-PVA electrospun fibrous membrane (R_0) and their resistance when exposed to 90 ppm NH_3 gas (R).

percent PANi (% wt/v)	Average diameter fiber (nm)	Resistance (MΩ) (n=5)		
		R_0	R	ΔR
2	387 ± 47	47.833	13.376	32.199
3	357 ± 52	49.068	10.986	38.082
4	446 ± 64	35.950	6.292	29.658
5	405 ± 59	38.566	10.750	27.816
6	363 ± 50	38.730	5.687	33.043

Table 4.4 summarized the electrical resistance of PANi-PVA fibrous membrane when exposed to ammonia gas. The electrical resistance of electrospun mat at various percent of PANi did not significantly different within studied. It might be caused by partly undissolved PANi or inhomogeneous of polymer solution before spinning process. However, the different in response time of the electrospun citric acid doped PANi-PVA mat at various percent of PANi was observed. The response time was decreased with increase in concentration of PANi from 2% to 5% wt/v as shown Figure in 4.13. However, PANi could not be perfectly dissolved in NMP and it affected the result of resistance and response time.

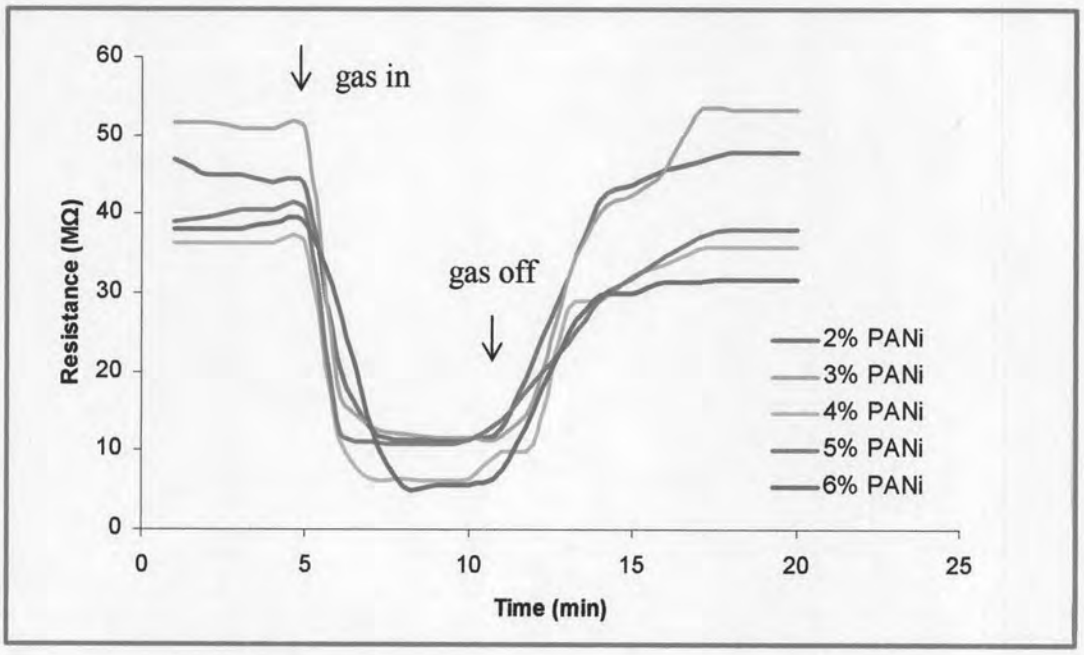

Figure 4.13 Resistance of electrospun citric acid doped PANi-PVA mats with different percent of PANi when exposed to 90 ppm of ammonia gas.

4.3.3 Effect of citric acid

From Table 4.5, it clearly demonstrated the change of fibrous membrane resistance when varied percent of citric acid. The resistance decrease when percent of citric acid increased. The possible reason was the increase in protonation of PANi with the acid resulting in the increasing imine sites. In other words, the more increase in percent of citric, the lower the initial resistance was.

Table 4.5 Resistance of PANi-PVA electrospun fibrous membrane (R_0) and their resistance when exposed to 90 ppm NH_3 gas (R).

Citric acid (g)	Resistance (MΩ) (n=5)		
	R_0	R	ΔR
0.6	84.49	N/A	N/A
1.2	48.81	13.40	35.41
1.8	35.77	23.16	12.61
2.4	8.290	6.090	2.200
3.0	8.653	6.716	1.937

N/A – not available

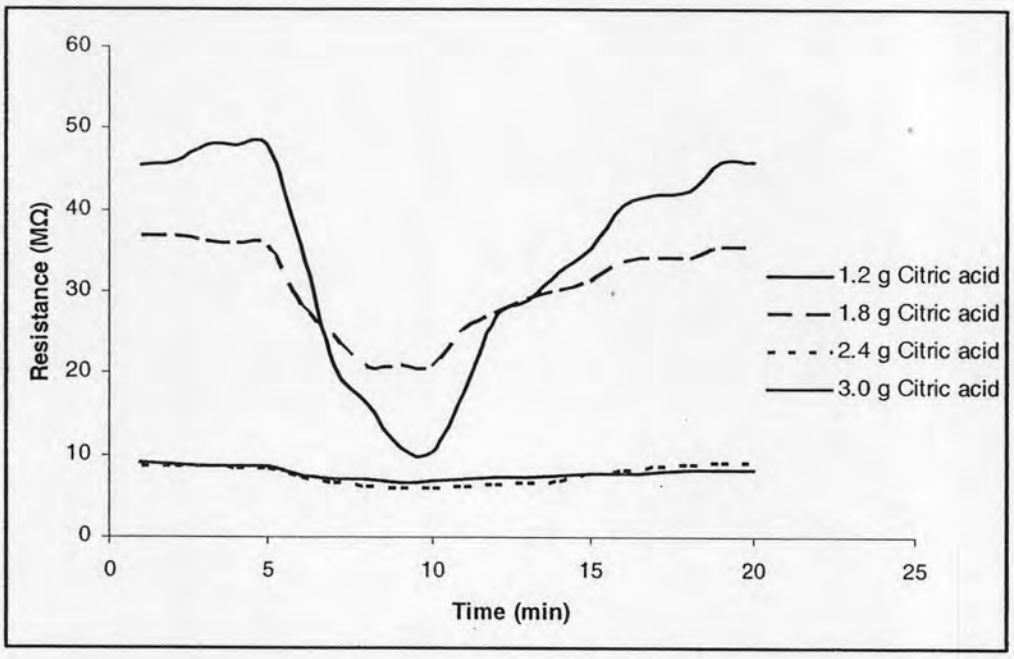

Figure 4.14 Resistance of electrospun citric acid doped PANi-PVA mats with different percent of citric acid when exposed to 90 ppm of ammonia gas.

Table 4.5 and Figure 4.14 showed the resistance of electrospun citric acid doped PANi-PVA mats on exposure to 90 ppm ammonia gas at 0.6, 1.2, 1.8, 2.4 and 3.0 g of citric acid doped. The initial resistance of electrospun mat with 0.6 g of citric acid doped was too high to be measured reliably with the set-up because the digital multimeter has a limitation of resistance detection. Therefore, this electrospun mat with 0.6 g of citric acid doped was not suitable for ammonia sensing. The electrospun mats with 2.4 and 3.0 g of citric acid doped was presented a slight change of resistance while with 1.2 and 1.8 g of citric acid doped resulted in a great change of resistance. However, change of resistance of PANi-PVA fibrous membrane with 1.2 g of citric acid-doped was more than that of PANi-PVA fibrous membrane with 1.8 g of citric acid. Therefore, 1.2 g of citric acid was chosen for better sensitivity.

4.3.4 Effect of solvent

The variation of solvents such as chloroform and acetone was studied to compare with NMP. Fibrous structures obtained from chloroform were uniform in diameter and straight comparing to those obtained from NMP and acetone as shown in Figure 4.15. The average diameter of PANi-PVA fibers using NMP as solvent was 509 nm which is smaller than those using chloroform (530 nm) and acetone (615 nm). The smaller fiber diameters resulted from jet extension because NMP has a high boiling temperature so the jet will have more time for the solvent to be evaporated. On the other hand, acetone that has a low boiling temperature was easy to evaporate. Therefore, fibrous structures were less uniform. The changing of fibrous membrane resistance were also studies. Change of resistance of electrospun mats obtained from chloroform was higher than that of electrospun from NMP and acetone as shown in Table 4.6. However, the initial resistance of PANi in NMP was lower than chloroform and acetone. In other words, PANi in NMP was resulted in a great conductance. It might be caused by mostly undissolved PANi in chloroform or acetone. Therefore, concentrations of PANi after filtration were not real and will have influence on measured electrical resistance.

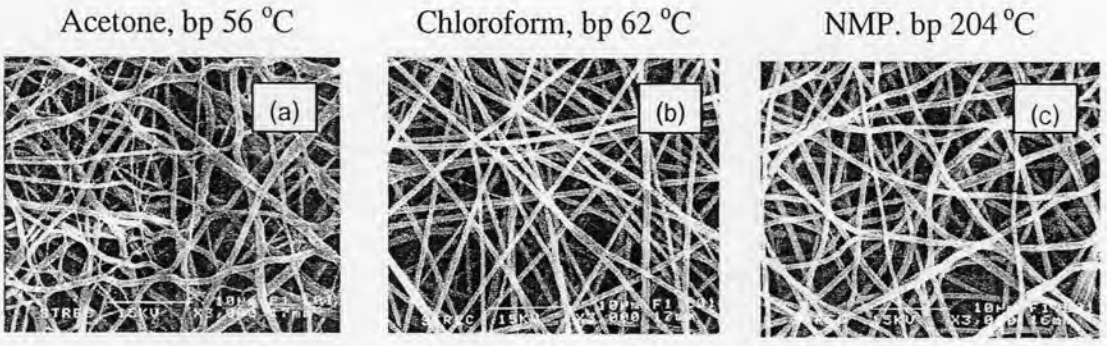

Fig.4.15 SEM of electrospun mats from 2 PANi % wt/v in (a) acetone, (b) chloroform and (c) NMP at solution flow rate of 15 μL/min, distance between needle and collection screen of 25 cm and electric potential of 15 kV. Original magnifications are 3,000x.

Table 4.6 Resistance of PANi-PVA electrospun fibrous membrane (R0) at different solvent and their resistance when exposed to 90 ppm NH_3 gas (R)

PVA : PANi (% wt/wt)	Solvent	Resistance (MΩ)		
		R_0	R	ΔR
97 : 3	N-methyl-2-pyrrolidone	7.024	5.231	1.793
97 : 3	Chloroform	78.808	27.098	51.710
97 : 3	Acetone	45.470	16.480	28.990

4.3.5 Response time and recovery time

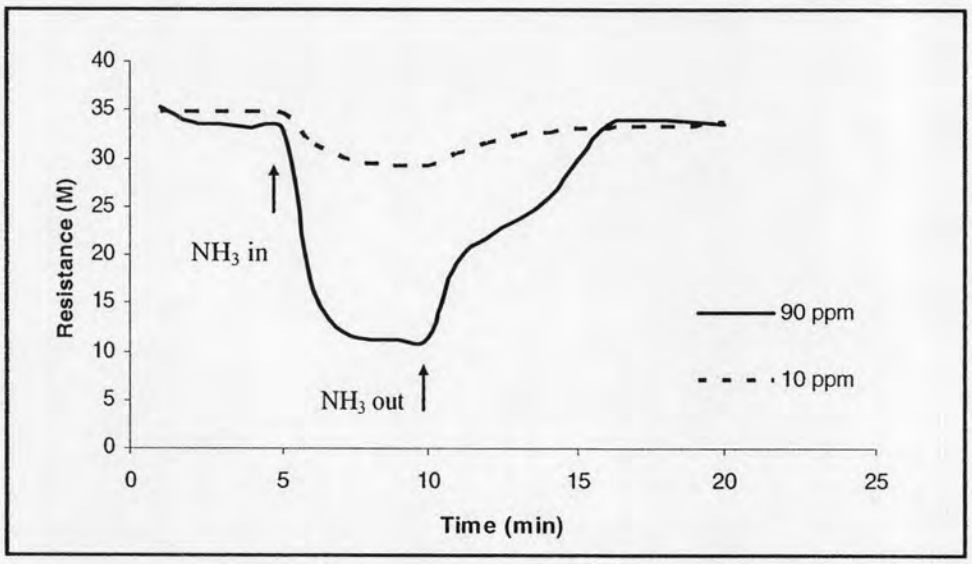

Figure 4.16 Response time and Recovery time of electrospun citric acid PANi-PVA mats when exposed to ammonia gas.

In order to determine the response time and the recovery time, the resistance of electrospun mats was monitored in a measuring chamber in which the resistance decreased and increased repeatedly. The response time of electrospun citric acid doped PANi-PVA mats was the time period that the resistance of the electrospun mat stopped changing on the exposure of ammonia gas. The recovery time was the time period that allowed the resistance of the electrospun mat returning to an initial

value after turn off the ammonia gas. Figure 4.16 showed the resistance of electrospun citric acid doped PANi-PVA mat for ammonia exposed at 10 ppm and 90 ppm. Both responses of fibrous membrane reached the equilibrium within 5 minutes. Therefore, the response time was set at 5 minutes. When the ammonia was turned off for fibrous membrane recovery, the resistance increased to the baseline after regeneration for 10 minutes. Hence, the recovery time was set at 10 minutes. This mechanism indicated electrospun citric acid doped PANi-PVA mat for ammonia sensing would be reversible. The response time of the electrospun citric acid doped PANi-PVA mat decreased with increase in concentration of ammonia gas from 10 ppm to 90 ppm. The increase of concentration enhances the rate of diffusion of ammonia molecules towards and into the fibrous membrane. The number of molecules that achieving contact with the sensing sites on the mat in a given time increase and therefore the response time decreases. The optimized response time of 5 minutes and recovery time 10 minutes were chosen to cover the range of working ammonia concentration, and for shortly and effectively repeating ammonia sensing.

4.3.6 Repeatability

Figure 4.17 showed the response of the electrospun citric acid doped PANi-PVA mat when repeatedly exposed to ammonia gas. The response of the electrospun mat was resulted in a similar value for 12 cycles continuously. However, the resistance was gradually decreased when repeatedly exposed to ammonia gas. The decrease of resistance would be resulted from the sorption of water molecule to PANi backbone or PVA backbone. This would affect the kinetic energy of ammonia molecule in the system. The water molecule favored the absorption of ammonia gas into electrospun mats and the ammonia molecules have low kinetic energy at low temperature, hence ammonia molecule in gas phase was unfavored. More ammonia molecules adsorbed on the electrospun mats. Therefore, the raising of water molecule in system would lead to a decrease of overall resistance.

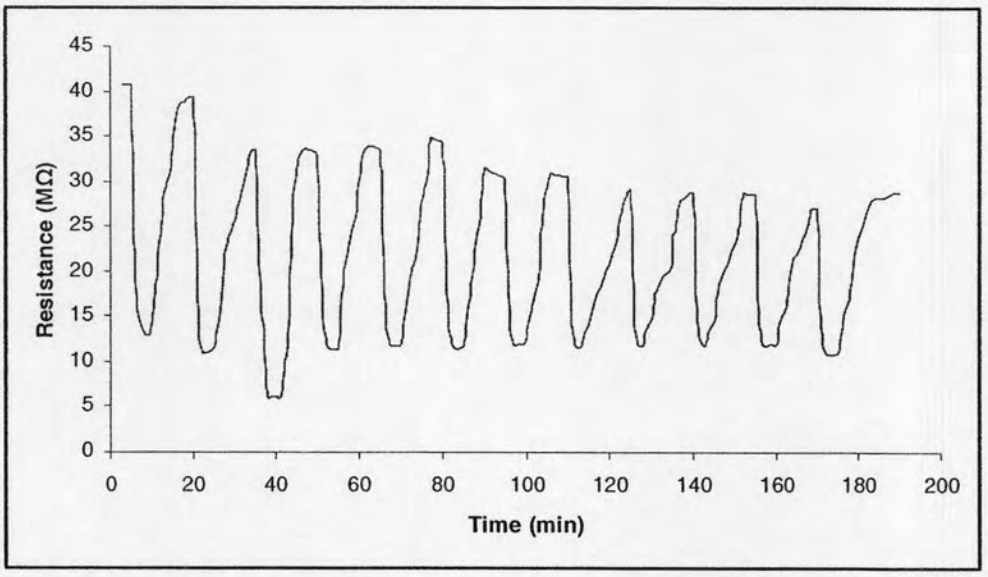

Figure 4.17 Response of electrospun citric acid doped PANi-PVA mats when repeatedly exposed to 90 ppm of ammonia gas.

Table 4.7 Repeatability of electrospun citric acid doped PANi-PVA mats when exposed various ammonia concentrations.

Cycle	ΔR (MΩ)				
	10 ppm	**30 ppm**	**60 ppm**	**90 ppm**	**100 pm**
cycle 1	5.411	11.740	18.640	28.386	32.668
cycle 2	5.587	11.115	18.040	27.571	33.223
cycle 3	5.350	11.991	18.650	27.655	32.862
average	5.449	11.615	18.440	27.871	32.918
SD	0.123	0.451	0.349	0.448	0.282
%RSD	2.260	3.875	1.893	1.607	0.857

Table 4.8 Repeatability of various sample of electrospun citric acid doped PANi-PVA mats when exposed to 90 ppm of ammonia gas.

Cycle	ΔResistance (MΩ)						
	Sample						
	1	**2**	**3**	**4**	**5**	**6**	**7**
1	28.690	25.340	28.386	25.650	28.260	25.690	27.540
2	30.710	26.061	27.571	26.810	26.340	24.640	28.130
3	29.210	25.063	27.655	25.960	28.180	25.030	29.620
average	29.537	25.448	27.871	26.140	27.590	25.120	28.430
average of various sample	27.163						
SD	1.637						
%RSD	6.02						

Table 4.7 showed the repeatability of the electrospun citric acid doped PANi-PVA mat when exposed ammonia in the range of 10 – 100 ppm. %RSD of electrical resistance response was ranged from 0.857 to 3.875%. It indicated a good precision of this sensor recommended by AOAC Peer Verified Methods (5.3% at 100 ppm and 7.3%. at 10 ppm). Moreover, the average change of resistance observed from various sample showed the similar results. %RSD of the change of resistance was 6.02% as shown in Table 4.8. It indicated a good precision and variation of samples did not significantly affect the resistance change of the electrospun mats sample. However, the irregular distribution of fibers on collector during spinning which result in the difference of mass of fibers and the limitation of life time of gold electrode might affect on resistance change of each electrospun mats sample. Moreover, temperature and humidity surrounding a sensor will also influent the ammonia detection capability of PANi-PVA electrospun mats.

4.3.7 Linearity

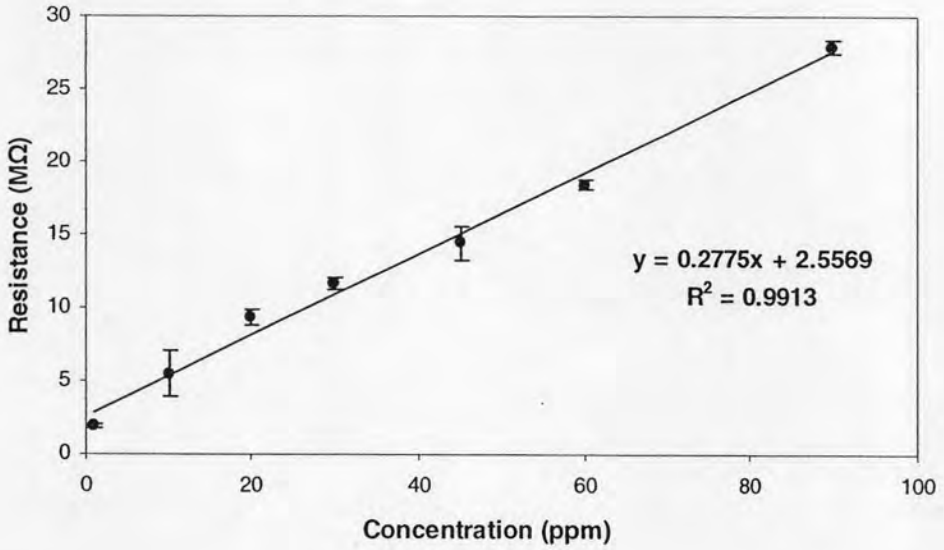

Figure 4.18 Resistance of electrospun citric acid doped PANi-PVA mat when exposed to different concentrations of ammonia gas.

Figure 4.18 showed the changes in the resistance of the electrospun citric acid doped PANi-PVA mat on exposure to ammonia gas concentrations in the range of 1 to 100 ppm. The linearity shows a correlation coefficient of 0.9913. This suggests that the PANi-PVA electrospun mats sensor can be reliably used to detect ammonia concentrations in this range.

4.3.8 Comparison of sensing capability between electrospun mats and cast film

The cast films were used to compare its ability of electric resistance to the electrospun mats. The change of resistance of electrospun PANi-PVA mats from electrospinning and PANi-PVA blend film fabricated by casting were 28.692 MΩ and 12.412 MΩ, respectively, when exposed to 90 ppm NH_3 gas as shown in Table 4.9. The initial resistance (R_0) of the electrospun PANi-PVA mats was lower than that obtained from PANi-PVA blend film at same PANi concentration. The result showed that the conductance of electrospun fibrous membrane was better than cast film. The resistance of PANi-PVA cast film decreased when exposed to ammonia gas and

reached the equilibrium after 5 minutes. When the ammonia gas was turned off for film membrane recovery, the resistance slowly increased to the baseline and need time for regenerate the cast film for more than 10 minutes. Recently, Chatuporn [14] has reported the response time and recovery time under NH_3 gas of citric acid doped PANi-PVA blend film fabricated by casting at same PANi-PVA concentration. When cast films were compared with the electrospun mats, the response time and recovery time of electrospun mats were faster. Due to the high porosity of the non-woven mat of electrospinning could be easily adsorption (high permeability for gases), hence, the change of resistance of electrospun was higher and also the response time was faster than those of cast film.

Table 4.9 Comparison of resistance, response time and recovery time of electrospun mats and cast film when exposed to 90 ppm of ammonia gas.

	Resistance (MΩ)		**Response time (min)**	**Recovery time (min)**
	R_0	**ΔR**		
Electrospun mats	32.954	28.692	5	10
Cast film	53.321	12.412	10*	20*

* Data from reference 14

4.3.9 Application in real sample

Table 4.10 Ammonia gas concentration determined in gaseous samples by using electrospun mat sensor and OLDHAM sensor

Site	**Ammonia concentration (ppm)**	
	Electrospun mat sensor	**OLDHAM Mx2100 sensor**
1	2	2
2	4	5

The electrospun mat sensor was applied for the determination of ammonia gas in gaseous samples and compared with the value obtained by OLDHAM Mx2100 sensor. The corresponding concentration of gaseous sample was calculated from the calibration equation in Figure 4.18. As shown in Table 4.10, the ammonia gas concentration using electrospun mat sensor of site 1 and site 2 were comparable to

those from OLDHAM Mx2100. It was observed that ammonia gas concentration obtained from electrospun mat sensor were a bit lower than those obtained from OLDHAM Mx2100. However, they were acceptable at this concentration level when compared with OLDHAM Mx2100 ammonia sensor. Therefore, electrospun mat sensor was successfully applied for determination of ammonia gas in gaseous samples and could be developed to commercial sensor.